Modeling and Evaluation of a Plug-In Hybrid Fuel Cell Shuttle Bus

C. S. Hearn, M. C. Lewis, R. C. Thompson, and R. G. Longoria

***Abstract*— The Center for Electromechanics at The University of Texas at Austin acquired a plug-in hybrid fuel cell bus for demonstration and model development under a program funded through the USDOT-FTA. The purpose of this program was to evaluate the performance and use of the bus while developing a model that could predict overall performance and energy consumption on daily driving routes. A model of the fuel cell bus was developed using PSAT (Powertrain Analysis Toolkit). The model development involved verifying component characteristics and a parametric study of drivetrain efficiencies to relate predicted to measured vehicle energy consumption data from on-road testing. The PSAT model was able to predict net energy consumption to within 5% over varying route profiles and vehicle conditions. Further investigations with advanced energy storage were performed to evaluate the benefits of ultracapacitor assisted batteries by using the correlated PSAT model. Ultracapacitors act as an additional load leveling device in the hybrid vehicle for peak propulsion and braking vehicle loads, thereby reducing stress on the batteries. The model simulation results show that ultracapacitors can increase overall vehicle economy by 2 to 4% and deliver a net increase in battery efficiency of 3 to 4%.**

***Index Terms*—Plug-In Hybrid Bus, PSAT, Ultracapacitor Battery Energy Storage , Vehicle Modeling,**

I. Introduction

UNDER a program funded through the USDOT – Federal Transit Administration, The Center for Electromechanics at The University of Texas at Austin acquired a 6.7 m long (22 ft.) plug-in hybrid fuel cell (PHFC) bus, manufactured by the Ebus Company in Downey Ca.

The program had two overall goals. The first goal was to evaluate the performance of the plug-in hybrid fuel cell bus and the technology behind it. The second goal was to develop a computer simulated model of the bus, using the Ebus data as a benchmark, which would provide a knowledge base for modeling heavy hybrid vehicles architectures; that is, develop a computer model of the Ebus which can be used to accurately predict performance for any given route.

The computer model of the PHFC bus was developed with PSAT (Powertrain Analysis Toolkit). PSAT is a forward looking software package developed by Argonne National Laboratories which utilizes Matlab and Simulink behind a graphical user interface. The Matlab and Simulink components in PSAT enable the user to modify vehicular components and control strategies to match observed vehicle characteristics.

Initial PSAT model results of the PHFC bus had been previously reported by Flynn *et al.* during initial model development [1]. Flynn *et al.* used PSAT to assess the impact of prime movers (hydrogen fuel cell or hydrogen internal combustion engine) and energy storage (NiCD batteries or flywheels) on the overall performance and energy consumption of the PHFC bus.

Related studies have been reported that compare vehicle performance predictions to test data. He *et al.* used PSAT to model a hydrogen ICE, parallel hybrid, Ford Explorer [2]. The PSAT model of the Ford Explorer included test data from hydrogen ICE dynamometer testing and relevant control strategies. The PSAT model was validated against chassis dynamometer testing of a converted Ford Explorer hydrogen ICE, parallel hybrid, which concluded the model accurately represented vehicle performance over long term analysis. It was found that dynamic sub-component models were required to better characterize battery and engine performance during transients. Although the PSAT model was successfully validated against in-laboratory test data, the model was not compared to on-road test results. On-road testing can introduce variations due to environmental conditions, for example, that can significantly influence vehicle performance.

The original PSAT model developed by Flynn *et al.* was created before the bus demonstration trials at The University of Texas and relied on initial understanding of the bus parameters and control strategies as reported by the vendor. This paper describes the testing and PSAT model development during the eight month bus demonstration period. During this time, the bus operated over three different routes, with different driving characteristics. Modifications were made to the component models and control strategies of the PHFC bus PSAT model so that the energy consumption predictions of the model would match those recorded by the bus during on-road test trials.

Not all individual components of the PHFC bus could be

This work was supported in part by the U.S. Department of Transportation Grant TX26710600

C.S. Hearn is with The University of Texas at Austin – Center for Electromechanics, Austin, TX 78758 USA (phone: 512-232-1637; fax: 512-471-0781; e-mail: Hearn@ cem.utexas.edu).

M.C. Lewis is with The University of Texas at Austin – Center for Electromechanics, Austin, TX 78758 USA (e-mail: mclewis@cem.utexas.edu).

R. C. Thompson is with The University of Texas at Austin – Center for Electromechanics, Austin, TX 78758 USA (e-mail: r.thompson@cem.utexas.edu).

R. G. Longoria is with The University of Texas at Austin – Department of Mechanical Engineering, Austin, TX 78712 USA (e-mail: r.longoria@cem.utexas.edu).

Fig. 1. Plug-in hybrid fuel cell bus manufactured by Ebus

isolated and uniquely characterized for incorporation into the PSAT model. This paper describes the method used to characterize vehicle components and use of parametric model studies to quantify hard-to-measure parameters, such as drive train efficiencies.

Once the correlated and benchmarked PSAT model of the PHFC bus was completed, a model-based investigation into design improvements was performed. Ultracapacitor assisted batteries are considered for potential performance improvements. Ultracapacitors are high power, energy storage devices, which can store and deliver the peak power needed during vehicle acceleration and regenerative braking to reduce current draw on the batteries.

II. Plug in Hybrid Fuel Cell Shuttle bus overview

The PHFC bus is shown in Fig. 1. The vehicle is powered by two parallel banks of NiCd batteries, which alone, give the bus a range of around 60 km. A 19.1 kW Ballard hydrogen fuel cell is used for range extension to recharge the batteries during operation. With the fuel cell, the bus range can be extended to 200 km. The shuttle bus is 6.7 m in length, has a gross vehicle weight rating of 8845 kg, and can seat up to 22 people. Table I shows a summary of the bus specifications.

The NiCd battery banks (Nickel – Cadmium) are the rechargeable energy storage source on the bus. The two battery banks consist of 50 6V, 100 Ah NiCd modules aligned in series, which yields a bus voltage of 300V. These batteries store a total of 60 kWh of energy, with 48 kWh usable at an 80% DOD (depth of discharge). Based on the manufacturer's specification sheet, these batteries can deliver up to 150 kW of power [3]. The batteries are charged overnight by a plug-in charger, but also recuperate energy from regenerative braking during operation. In addition to providing significant energy storage for the shuttle bus, these batteries add a significant amount of mass to the bus. The batteries alone add 1320 kg to the vehicle mass, with an addition 640 kg for the support casing.

A 19.1 kW Ballard fuel cell provides extra energy and power during operation to maintain the SOC (State of Charge) of the NiCd batteries. Up to 12.8 kg of compressed hydrogen is stored in two roof mounted, composite tanks at 5000 psi. The hydrogen fuel cell is programmed to start producing power when the battery SOC has fallen below 65%. To protect the batteries from overcharging, and improve regenerative braking performance, the fuel cell will turn off and stop producing power if the battery SOC increases to 75%.

Table I. Bus specifications

Vehicle	**Fuel Cell Shuttle Bus**
Bus Manufacturer	Ebus Inc.
Year Model	2007
Length/Width/Height	6.7 m / 2.3 m / 2.8 m
Ground Clearance	20 cm
Wheel Base	3.7 m
GVWR	8845 kg
Passengers	22 seated
Power Plant and Manufacturer	19.1 kW PEM Fuel Cell / Ballard
Fuel	12 kg - Compressed Hydrogen
Fuel Storage	2 5000 psi Roof mounted tanks
Hybrid Type	Series/Charge depleting
Energy Storage	NiCD Batteries
Manufacturer / Model	Saft / STM5-100MRE
Total Energy Storage	60 kWh
Propulsion Motor/Manufacturer	Induction Motor / Reliance Electric
Nominal/Peak power	75 kW / 130 kW for 1 min
Nominal/Peak torque	400 Nm / 700 Nm for 1 min
Transmission	Chain Drive/rear differential
Regenerative Braking	yes

The shuttle bus drivetrain is powered by a 75 kW induction motor, linked by a single reduction chain drive to the drive shaft and differential. This motor has a nominal continuous output torque of 400 Nm, and can produce a peak torque up to 700 Nm, and 130 kW peak power for 1 minute. The traction motor performance limits the maximum vehicle speed to 70 km/hr. This traction motor also serves as a generator when braking to recharge the batteries which improves overall vehicle economy.

III. Route Descriptions

The PHFC bus performance was demonstrated over three different routes in the Austin area between October 2007 and May 2008. Three routes were selected to demonstrate different operating modes and abilities of the bus. Expanding the operating realm of the bus also increased the model validity since the correlated computer model would have to predict bus performance over different terrain, speed ranges and stop frequencies. From November 2007 to March 2008, the bus ran the selected routes on battery power alone to isolate one side of hybrid operation for performance evaluation and model correlation. During April and May of 2008, the bus operated the routes under full hybrid operation, which included the use of the hydrogen fuel cell for range extension. The PSAT bus model was updated to correlate the bus operating in hybrid mode.

Table II. Route properties

Route	PRC Campus	Great Hills Route	Jollyville Parmer
Length [km]	3.1	12.0	17.9
Average Speed [km/hr]	4.0	7.3	7.4
Highest Grade [%]	1.5	13.0	6.0

The three different demonstration routes selected during the evaluation period are referred to as:

- PRC Campus Route - Low speed, flat, and frequent stops
- Great Hills Route - Moderate speed, very hilly, and moderate stops
- Jollyville Parmer Route – High speed, some hills, and infrequent stops

The PRC Campus route is a 3.1 km loop around the Pickle Research Campus at The University of Texas at Austin. This route is relatively flat and low speed, with a top speed of 40 km/hr. Eight simulated "bus stops" were designated along the route with a spacing of a quarter to half a kilometer between each one. This low speed route is ideally suited to the lower-powered shuttle bus. During the hybrid mode demonstrations with fuel cell operation, the fuel cell was able to maintain the battery SOC along the route.

The next route selected was the Great Hills Route. This route was 12 km in length and operated through a significantly hilly residential area of northwest Austin TX. The speeds on this route reached up to 56 km/hr, but stayed mostly around 30 to 40 km/hr. This route had a total change in elevation of 70 m, with grades that exceeded 10% in some areas. Due to the hills, this route exhibited significantly higher power consumption than the flatter and slower PRC Campus route. During fuel cell operation, the batteries on the bus would discharge before all available hydrogen was consumed, although at a slower rate than battery power alone. In order to correlate bus performance to computer model prediction, the elevation along this route was recorded with an altimeter and incorporated into the PSAT models.

The last route demonstrated was the Jollyville Parmer route, which ran on higher speed roads in the Northwest Austin area. This route was 17.9 km in length and reached maximum bus speeds of 70 km/hr. This route did have the same 70 m elevation swing as the Great Hills route, but these changes occurred over greater distances and the grades were generally less than 5% along the route. Like the Great Hills Route, the vehicle power requirements along this route tended to drain the batteries faster than the fuel cell could recharge them and a constant SOC operating point was not maintained. Table II shows a summary of the three different demonstration routes.

IV. Model Development

PSAT was used for model development and correlation. The vehicle configuration setup of a fuel cell series hybrid bus in PSAT is shown in Fig. 2. The fuel cell connects to the main battery bus via a DC/DC boost converter. The 60 kWh NiCD battery bank battery powers the traction motor minus the auxiliary loads. Typical vehicle dynamic equations are then used in PSAT to calculate motor torque requirements, vehicle losses from grade, rolling resistance, and aerodynamic resistance, as the vehicle power requirements are simulated along the route.

Although PSAT offers a large library of component models, such as batteries, traction motors, and vehicle bodies, which have been collected by research and testing at Argonne National Labs, these models may not always accurately represent the components on a specific vehicle. For model correlation with the PHFC bus, the correct data was required to accurately characterize the vehicle performance. The first phase of model correlation focused on the "Battery" operation mode of the shuttle bus where two primary methods were used to fill in the model parameters. The first method relied on vendor supplied data which provided information on gear ratios, vehicle mass, vehicle drag coefficient, battery bank size, and the traction motor torque/speed characteristics. The second method relied on observing bus performance and correlating the PSAT model to match these results. In this latter process, traction motor characteristics were reevaluated and parametric studies on overall drivetrain efficiency were performed. Once the model had been correlated to "All Battery" mode results, fuel cell operation, based on stand-alone testing, was included into the PSAT model. This final model was then correlated to bus performance data during full hybrid operation.

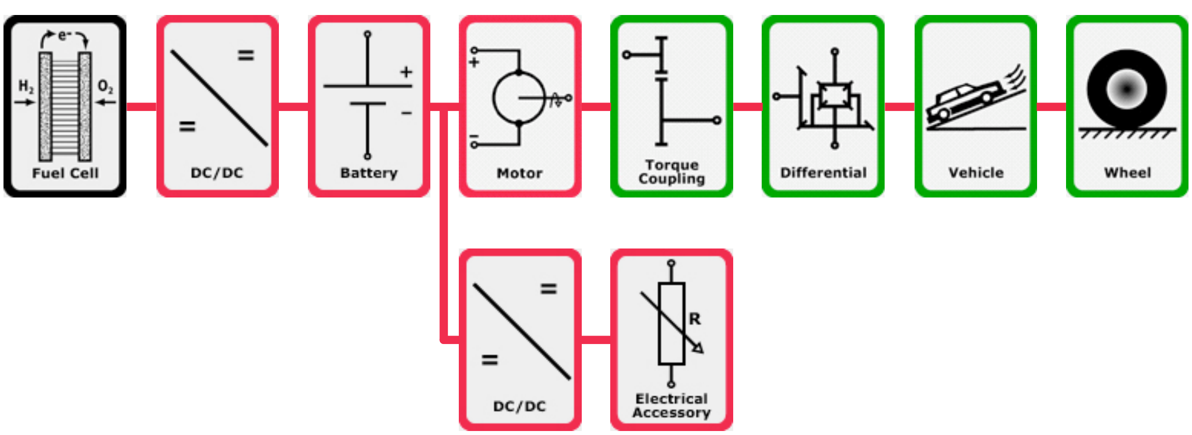

Fig. 2. PSAT Model layout for series hybrid fuel cell bus

To compare model performance predictions to recorded data, the route profile (speed vs. time) for each respective data set is used as a model input, so that the PSAT model simulates the bus following the route the actual bus completed on a particular day. The recorded auxiliary loads from the respective data sets are also included as model inputs. The auxiliary load on the PHFC bus can range between 3 kW to 10 kW, depending on whether or not the A/C system is operating. Since this large change in power consumption can have significant effects on end energy use, the model uses the recorded power profile to put emphasis on accurately modeling the complete powertrain performance (fuel cell, traction motor, drivetrain, road loads, etc…).

A. Battery Mode Modeling

To limit the variables present in model development, the bus initially ran the three demonstration routes, PRC Campus, Great Hills, and Jollyville Parmer, on battery power alone. The measured results during these demonstration trials were compared to the PSAT model results to guide model development. This measured data included vehicle speed, route tracking capabilities, and net energy consumed from the batteries. Initially all model parameters were determined from vendor supplied data sheets and performance specifications from the bus manufacturer.

Initial model results showed that there were discrepancies between vehicle speed capabilities as predicted by the PSAT model compared to results obtained from data on the higher speed Great Hills and Jollyville Parmer routes. The initial PSAT model used torque/speed curves supplied by the motor manufacturer which showed significant drop-off in torque and power capability at higher shaft rpm, as indicated in Fig. 3. Using this motor characterization, the initial PSAT model predicted that the PHFC bus could not maintain the speeds that had actually been recorded on a given route, notably at higher vehicle speeds, Fig 4. To correct this route tracking discrepancy, further analysis compared the traction motor power consumption over various routes, as recorded by the bus, to the maximum power from the vendor supplied torque/speed curves. This analysis showed that the traction motor was able to produce more power than what the vendor had originally specified, Fig. 5. In order to correct the traction motor model, new power curves were generated that envelop the observed traction motor power capabilities as recorded by the bus. This updated motor model still showed decreased

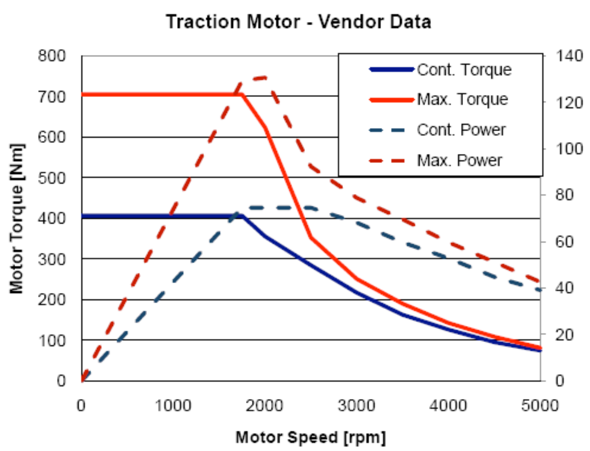

Fig. 3. Traction motor torque/speed curves as originally supplied by vendor

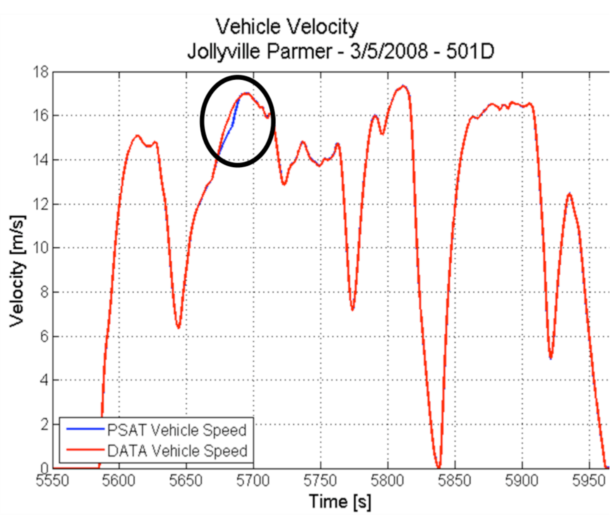

Fig. 4. Discrepancy between vehicle speed as predicted by the PSAT model (blue) to speed recorded by bus (red) over a section of the Jollyville Parmer route

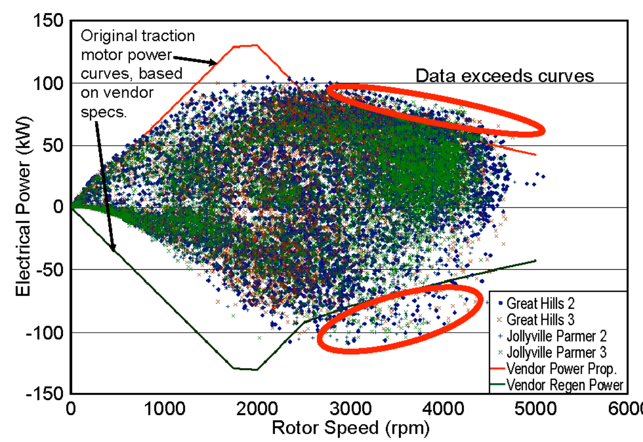

Fig. 5. Comparison of traction motor power consumption from recorded data (scatter plot) to original motor characteristic curves

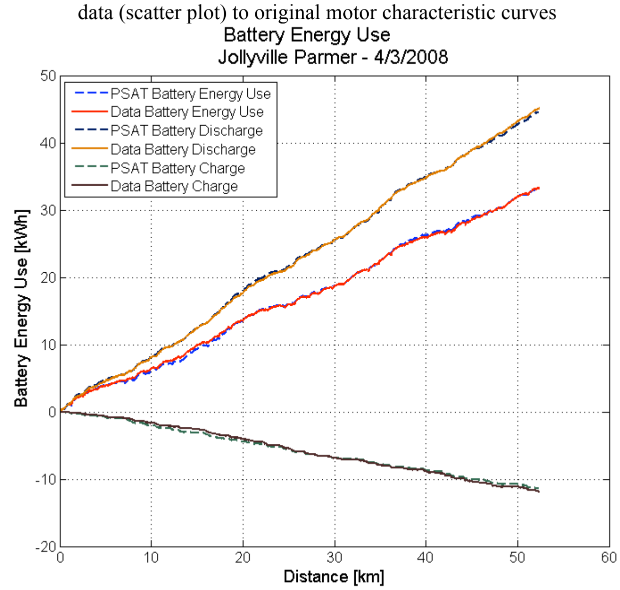

Fig. 6. Comparison of energy use between model and recorded data

power capability above rated speed, but not as severe as the initial vendor supplied data. With the updated motor model, discrepancies between measured and predicted vehicle speed were alleviated.

The drivetrain efficiencies through the traction motor, chain drive, and differential quantify key loss effects that significantly impact net energy consumption. Since there was no direct way to measure drivetrain efficiency, parametric studies of the PSAT model were performed. These studies involved adjusting the efficiencies of the chain drive and final drive in order to observe the effect on overall vehicle energy consumption, as measured by net battery energy consumed. The traction motor efficiency characteristics were kept constant throughout this study, which assumed the traction motor followed a typical induction motor efficiency map as supplied in the PSAT library.

For the drivetrain parametric study, the performance of the PSAT model was compared to 13 different sets of battery mode data collected over the three different demonstration routes with three different "payloads". The payloads represent an empty bus (0 kg), a half full bus, (756 kg), and full passenger load (1512 kg). The three sets of overall drivetrain efficiencies (through the chain drive and differential) used in the study were 87.3%, 85.5% and 83.7%. This study compared the net energy usage of the batteries as recorded from the route data to the value predicted by the PSAT model. Fig. 6 shows an example comparison of battery energy use over the route as predicted by the PSAT model and recorded by the bus computer. The battery discharge energy accounts for the bus propulsion and auxiliary requirements, while the charge energy accounts for energy recuperated during regenerative braking.

Table III and Fig. 7 show the results of this parametric study. This parametric study shows that selecting an overall drivetrain efficiency of 85.5% yields the best results by minimizing the difference between the measured and predicted net energy consumed by the batteries. With the higher drivetrain efficiency, the PSAT model tends to underestimate the amount of energy consumed by the batteries, and overestimates the energy consumed with the lower drivetrain efficiency. At an efficiency of 85.5%, the PSAT model of the shuttle bus can predict net energy consumed by the batteries to within 4%.

Table III. Comparison of net battery usage as predicted by PSAT model to recorded data by a parametric study on drivetrain efficiencies

		Recorded data	**Net Drivetrain efficiency 87.3%**		**Net Drivetrain efficiency - 85.5%**		**Net Drivetrain efficiency - 83.7%**	
	Payload	**Net Battery Usage [kWh]**	Net Battery Usage [kWh]	**Net Difference [%]**	Net Battery Usage [kWh]	**Net Difference [%]**	Net Battery Usage [kWh]	**Net Difference [%]**
PRC Campus	0 kg	**33.69**	31.85	**-5.5%**	33.21	**-1.4%**	34.6	**2.7%**
	756 kg	**38.91**	36.37	**-6.5%**	37.91	**-2.6%**	39.48	**1.5%**
	1512	**39.55**	38	**-3.9%**	39.5	**-0.1%**	41.04	**3.8%**
Great Hills Route	0 kg	**35.54**	34.37	**-3.3%**	35.77	**0.6%**	37.19	**4.6%**
	756 kg	**37.59**	35.63	**-5.2%**	36.97	**-1.6%**	38.32	**1.9%**
	756 kg	**32.59**	31.84	**-2.3%**	32.93	**1.0%**	34.05	**4.5%**
	1512 kg	**30.27**	30.09	**-0.6%**	31.29	**3.4%**	32.51	**7.4%**
	1512 kg	**29.4**	29.35	**-0.2%**	30.51	**3.8%**	31.7	**7.8%**
Jollyville Parmer Route	0 kg	**33.45**	31.18	**-6.8%**	32.32	**-3.4%**	33.45	**0.0%**
	756 kg	**38.95**	38.87	**-0.2%**	40.24	**3.3%**	41.48	**6.5%**
	756 kg	**31.68**	30.15	**-4.8%**	31.22	**-1.5%**	32.29	**1.9%**
	1512 kg	**32.59**	32.49	**-0.3%**	33.6	**3.1%**	34.75	**6.6%**
	1512 kg	**33.23**	32.11	**-3.4%**	33.21	**-0.1%**	34.34	**3.3%**

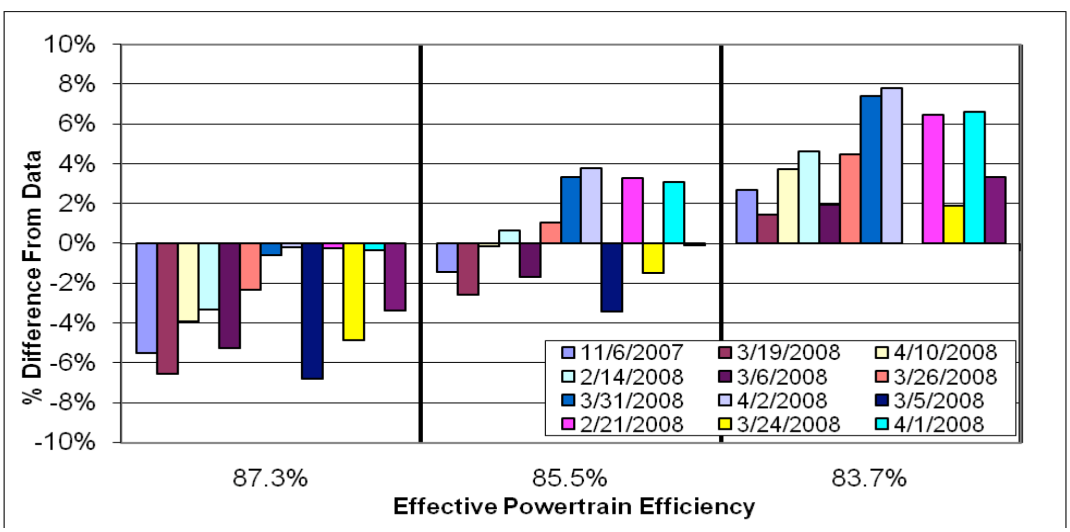

Fig. 7. Difference between net battery energy predicted by model and recorded data by parametric study on drivetrain efficiencies

B. Fuel Cell Modeling and Control

Once model correlation to the "All Battery" cases was completed, the PSAT model of the PHFC bus was updated to include fuel cell operation. Data from stand alone testing of the fuel cell was incorporated into the PSAT model, along with a simplified algorithm to replicate the fuel cell power commands of the bus software. This new model was correlated against 10 different data sets collected over the three test routes with different simulated passenger loads.

A test of the fuel cell power plant was performed to map fuel cell characteristics. The fuel cell system was tested by commanding different power levels from 15 kW to 3 kW in 3 kW increments. At each power increment, the fuel cell operated from 20 to 30 minutes so an accurate measurement of hydrogen consumption could be obtained. Longer dwell times were used for lower power levels since hydrogen consumption (i.e. kg/hr) was reduced. The data recorded by the bus computer was used to calculate the stack efficiency and BOP (Balance of Plant) losses at each power level for the fuel cell system.

Fig. 8 shows the raw data collected from fuel cell testing. The "Fuel Cell Stack Power" is the power coming from the fuel cell stack, which is calculated by multiplying the stack voltage and current. The "Fuel Cell Net Power" is the useful power out of the fuel cell power plant to the batteries, which is calculated and recorded by the bus computer. The "BOP Power Consumption" is calculated by the difference between the "Fuel Cell Stack Power" and the "Fuel Cell Net Power". The "BOP Power Consumption" represents the fuel cell Balance of Plant, and includes the parasitic loads consumed by the pumps, air compressors, and boost converter losses.

Data collected from testing was averaged over the constant power test periods and used to generate performance maps that were incorporated into the PSAT model. These maps reference the fuel cell stack power to BOP losses and hydrogen consumption as shown in Fig. 9. In the PSAT model, a command is given to the fuel cell for a specific stack power. The net power out and hydrogen consumption is then calculated by these maps.

A simplified algorithm is used to model the fuel cell power

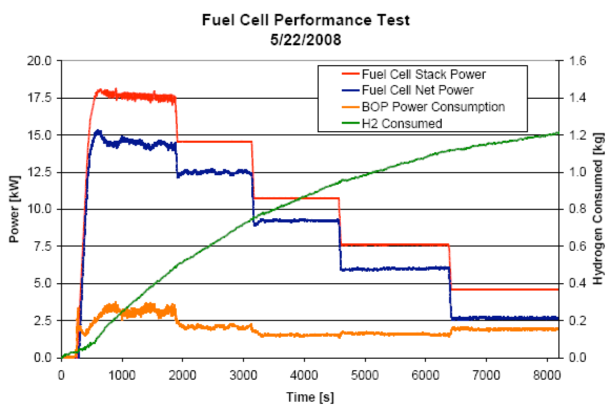

Fig. 8. Test results from stand-alone testing of fuel cell comparing stack power, hydrogen consumption and losses.

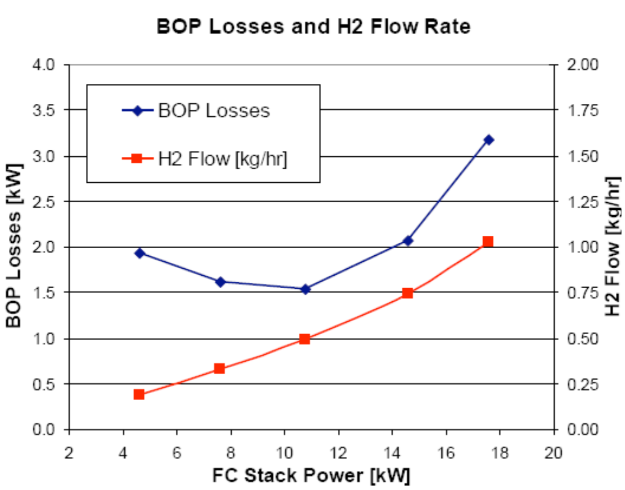

Fig. 9. Fuel cell stack power versus hydrogen consumption and losses for PSAT model

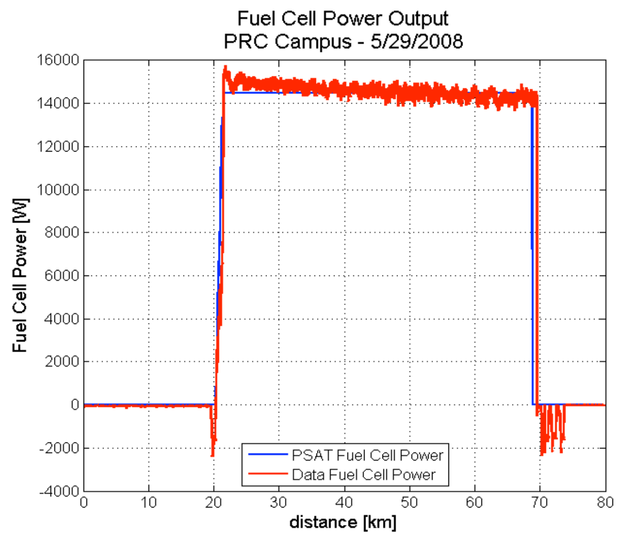

Fig. 10. Comparison of fuel cell output power as predicted by the PSAT model (blue) and results from recorded data (red)

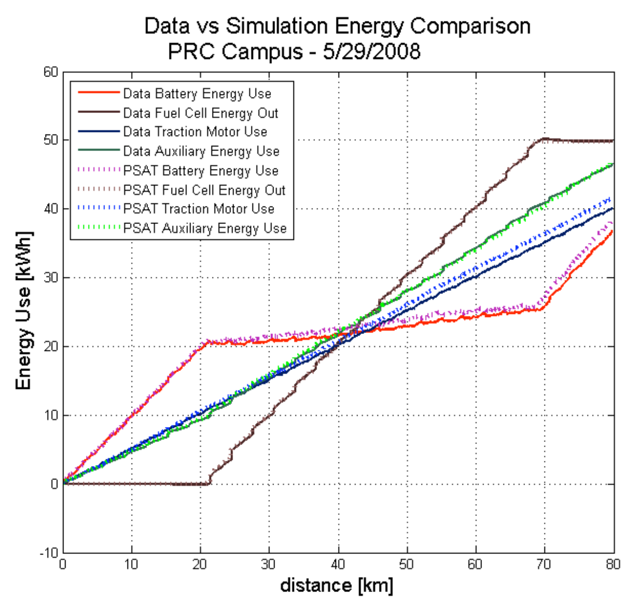

Fig. 11. Comparison of component energy consumption between PSAT model and recorded data

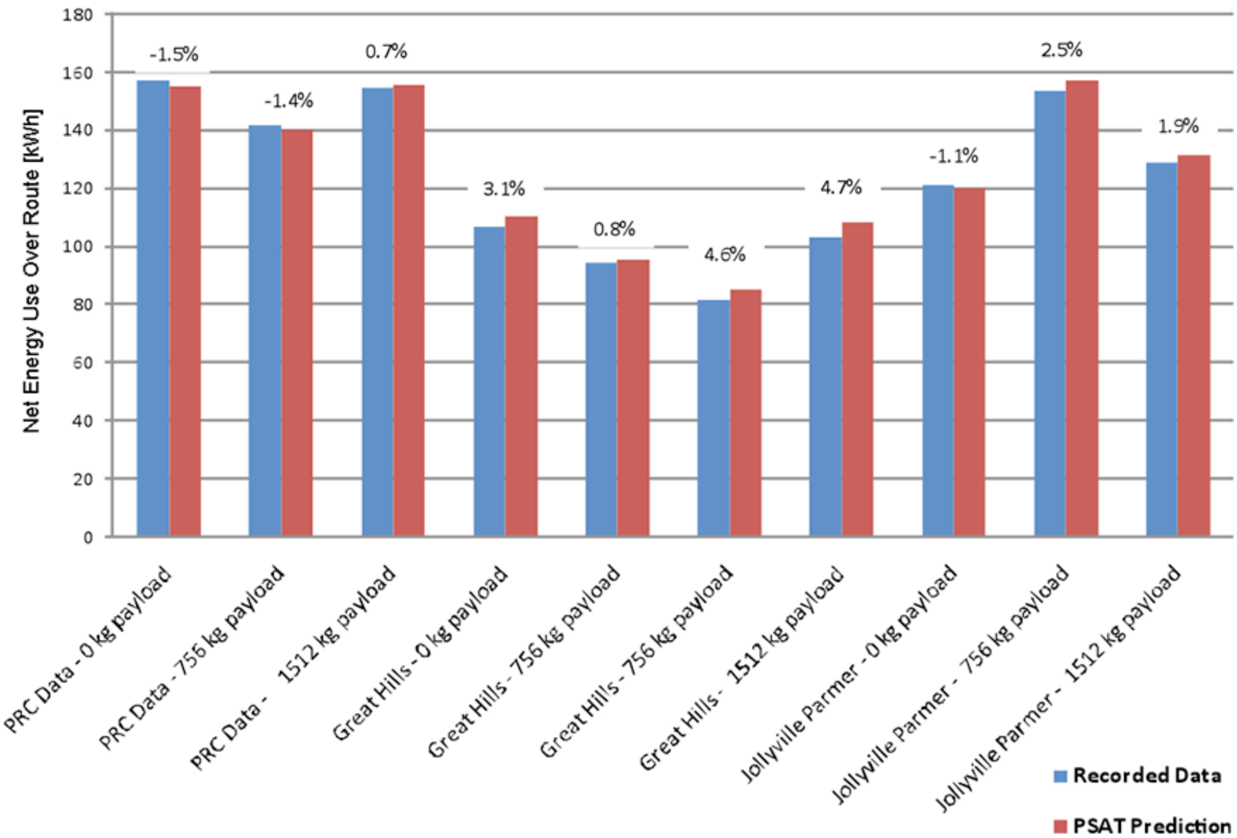

Fig. 12. Comparison of net energy consumed (from battery depletion and hydrogen consumption) as predicted by the PSAT model and recorded from the shuttle bus over the demonstration routes. Percent differences between predicted and recorded are shown above the bars.

request calculation that is performed by the bus computer. When the battery SOC falls below 65%, the controller commands the fuel cell to start producing power per Eq. (1). If the battery SOC rises to an upper limit of 75% from fuel cell recharging, the fuel cell shuts down to prevent damage to the battery. In Eq. (1), the SOC is the battery state of charge, L_{soc} is the upper limit for recharging (75%), P_{avg} is a rolling average of the traction motor and auxiliary power consumption, K is a gain value calculated by the bus manufacturer based on certain operating elements of the battery bank and size, and P_{fc_max} is the maximum power the fuel cell stack can deliver. In the actual bus computer algorithm, P_{fc_max} is calculated from a complicated algorithm based on fuel cell stack pressures and temperatures to ensure optimal stack operation. For the PSAT model, the value of P_{fc_max} is arbitrarily set to 17.5 kW, which is generally the maximum stack power that has been observed from the current demonstrations.

$$P_{fc} = \min\left[\left(K\left(L_{soc} - SOC\right) + P_{avg}\right), P_{fc\_\max}\right] \quad (1)$$

During the month of May 2008, the Ebus re-ran the three different demonstration routes in full hybrid mode with the fuel cell. During this demonstration period, 10 daily routes were selected to compare the model performance. Compared to the data collected during the battery-only model development, the bus generally traveled twice the distance along the demonstration routes due to the range extension capability of the fuel cell. Due to fueling limitations from the hydrogen supply source, only 4.8 – 5 kg of hydrogen could be stored in the tanks as opposed to the 12.8 kg of hydrogen the tanks were designed to store. Depending on the average vehicle power required to drive a specific route, this limitation reduced the overall distance traveled. For the low power routes, such as the PRC Campus, the fuel cell is able to maintain the battery SOC, therefore when the hydrogen is depleted, the batteries will start to run out. For the higher power routes, such as Great Hills and Jollyville Parmer, the fuel cell is unable to maintain the battery SOC, but the fuel cell does slow the depletion rate.

An example comparison of model results to recorded data over a demonstration route is shown in Fig. 10 and Fig. 11. These figures show the bus performance over the lower speed PRC campus route where the fuel cell is able to adequately supplement the vehicle road load. Fig. 10 shows the fuel cell power output from the model compared to the recorded data. The battery SOC reaches 65% after 20 km which triggers fuel cell operation. At approximately 70 km, the hydrogen fuel is exhausted and the bus continues along the route powered by the batteries alone. Fig. 11 tracks the component energy consumption along the route. This includes energy that is produced by the fuel cell (from net output power) and consumed by the traction motor, auxiliary loads, and overall net battery use.

To adequately compare the total energy use predicted by the PSAT model to the actual energy use recorded from the PHFC bus, the total energy consumed by the fuel cell and batteries must be considered. This net energy can be calculated by summing the net energy consumed by the batteries, E_{batt}, and the net chemical energy of the hydrogen gas consumed by the fuel cell, as shown in Eq. (2). The net chemical energy of the hydrogen gas is calculated by multiplying the lower heating value of hydrogen (LHV_{h2}) by the mass of the hydrogen consumed (M_{h2}). Fig. 12 shows a comparison of the net energy consumed as predicted by the PSAT model of the PHFC bus, to data recorded from the bus over the ten demonstration routes performed with fuel cell operation.

$$E_{sum} = E_{batt} + LHV_{h2} \cdot M_{h2} \tag{2}$$

These results show that the PSAT model is able to predict the net energy consumption to within 5% over the different routes and driving profiles. This result is similar to the 4% error band experienced by battery only operation. Potential sources of error can include outside factors such as wind or road conditions which affect road loads, in addition to further uncertainties in the traction motor and drivetrain efficiencies. Overall, the ability to accurately predict vehicle energy consumption and potential range to within 5% can yield useful information to determine the vehicle’s suitability for a potential route or explore the effect of design changes on energy storage or prime movers.

V. EBUS ENERGY STORAGE UPGRADES

To further investigate potential improvements to the PHFC bus, advanced energy storage concepts were investigated and simulated with the correlated PSAT model. One possible improvement is to add ultracapacitors to assist load leveling capabilities [4]. Ultracapacitors act as high power energy storage devices with power densities ten times greater than conventional batteries but less than a tenth of the energy storage capabilities of conventional batteries [5, 6]. For a battery-dominant? hybrid vehicle architecture, ultracapacitors can efficiently help to meet the peak power load requirements during acceleration and regenerative braking. This advanced load leveling reduces the current load on the batteries which can;

- Decrease ohmic losses and heating
- Increase battery life through reduced heating
- Increase overall energy storage efficiency

Studies performed by Park *et al.* [7] and Baisden *et al.* [8] have shown that ultracapacitors reduce the stress on batteries, provide potential to decrease the battery bank size, and can improve overall vehicle economy by 2.7%.

To evaluate performance improvements, the evaluation considered adding four 125 V Maxwell ultracapacitor modules to the 60 Wh NiCD battery bank. Specifications for the 125 V modules are described in Table IV. The total available energy delivered by the four 125 V ultracapacitor modules is approximately equal to the kinetic energy of the shuttle bus at maximum speed. Therefore the ultracapacitor bank should store enough energy to accelerate the bus to maximum speed.

A. Power Management Control Strategy

In order to incorporate ultracapacitor energy storage into the PSAT model of the PHFC bus, a power management control strategy must be implemented to direct power demands between the fuel cell, NiCd batteries, and ultracapacitor modules. In a real world application, power electronics would be used to control voltage and current demands between the energy storage devices. These demands would be dependent upon an overall power management strategy [9]. For this analysis, the power electronics are assumed to be ideal and lossless, and the focus is on the power management strategy.

The power management control strategy developed for the PHFC bus model uses a simplified analytical methodology which directly calculates how much power each device supplies based on load requirements and the states of the energy storage devices. Similar control strategies have been presented before by Napoli *et al.* [9] and Rosario and Luk [10] to manage power between an ultracapacitor and battery energy storage combination.

For the new power management control strategy, the fuel cell control strategy remains the same as described in Eq. (1) and is solely dependent on the SOC of the NiCd batteries. No changes were made to this control strategy since the maximum output power of the fuel cell is low and the fuel cell generally operates at maximum power during the previous analyzed routes. This decision directed the focus to power management between the ultracapacitor bank and NiCd batteries to supply the remaining vehicle power demand.

Fig. 13 shows a general schematic of the power management strategy between the NiCd battery and ultracapacitor bank. The battery bank supplies a specified, saturated, percentage of the vehicle power load, P_Load, plus an additional amount to ensure the ultracapacitor bank is near a specified reference voltage, V_oc_ref. The method used to calculate the ultracapacitor reference voltage, V_oc_ref, is modified from an approach described by Luk and Rosario [10] and is based on the vehicle kinetic energy, energy stored in the ultracapacitor, and correction terms that account for the fact that the maximum kinetic energy that the shuttle bus can attain may be higher or lower than what the ultracapacitors can deliver. This reference voltage ensures that the ultracapacitor bank is at full voltage when the vehicle is stopped, and at half voltage when the vehicle is at full speed. The ultracapacitor bank then delivers the remaining power requirements to meet the vehicle load demand.

Table IV. Specifications for Maxwell 125 V ultracapacitor module [ref]

	Unit	Value
Nominal Operating Voltage	V	125
Nominal Capacitance	F	63
DC Series Resistance	Ohms	18
Energy Available	Wh	59.5
Maximum Continuous Current	Amps	150
Lifetime	Cycles	1,000,000

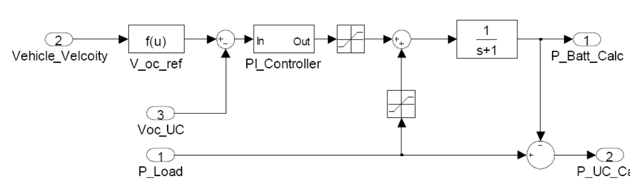

Fig. 13. Simplified schematic of power management control between the battery and ultracapacitor.

B. *Ultracapacitor Battery Analysis*

The PHFC bus with ultracapacitor battery energy storage was simulated over the low speed/low power PRC Campus route and higher speed/higher power Jollyville Parmer route. The analyses assumed four Maxwell ultracapacitor modules are added to the current NiCd battery bank with the previously discussed power management control strategy.

Fig. 14 shows a summary of performance improvements with the additional ultracapacitors over the standard NiCd battery bank. On the lower speed PRC Campus route, the additional ultracapacitors yield close to a 5% improvement in range while there is less than a 1% improvement in range on the higher speed Jollyville Parmer route. The lack of range improvement on the higher power Jollyville Parmer route is due to the inability of the fuel cell to maintain battery SOC along the route.

Improvements in overall vehicle economy are 2.6% and 2% on the PRC Campus and Jollyville Parmer route, respectively. These results are in line with those previously presented by Park *et al.* and Baisden *et al*. Further improvements in overall vehicle economy could be attained by reducing the size of the NiCd battery bank, and hence lower the vehicle mass, but this change would diminish the vehicle range.

Finally, net improvements of 3% and 4% in NiCd battery round trip efficiency are attained on the PRC Campus and Jollyville Parmer route respectively. These improvements in battery efficiency are a direct result of the reduced current load on the NiCd battery bank. Larger improvements on the higher power route are due to the original higher power demands on the NiCd battery bank.

VI. Conclusions

The fuel cell hybrid shuttle bus demonstration was completed on realistic transit routes in Austin, TX from October 2007 through June 2008, to evaluate some of the vehicle's advanced transportation technologies. The PHFC bus was operated on pre-determined routes to collect performance data.

The program had two overall goals. The first goal was to evaluate the performance of the plug-in hybrid fuel cell bus and the technology behind it. The second goal was to develop a computer simulated model of the bus, using the Ebus data as a benchmark, which would provide a knowledge base for modeling heavy hybrid vehicle architectures. This model was developed without any isolated sub-component testing to uniquely characterize the individual drive components of the powertrain, but rather relied on a method involving observation and parametric study of the overall vehicle system in order to characterize component behavior. This technique yielded a modeling and simulation basis capable of providing results matching actual energy consumption performance to within 5% of measured data from on-road testing.

Once the final correlated model was completed and benchmarked, the model could serve as a tool to analyze predicted bus performance on new routes or to evaluate improved performance with advanced energy storage and prime movers. To demonstrate this analysis capability, bus performance with ultracapacitor battery energy storage was assessed. It was shown that the addition of ultracapacitors reduced current draw and stress on the NiCd battery pack, leading to more efficient drivetrain operation. Analysis results showed range improvements of up to 5%, depending on the severity of the route and net efficiency improvements of the NiCd batteries by 3-4%.

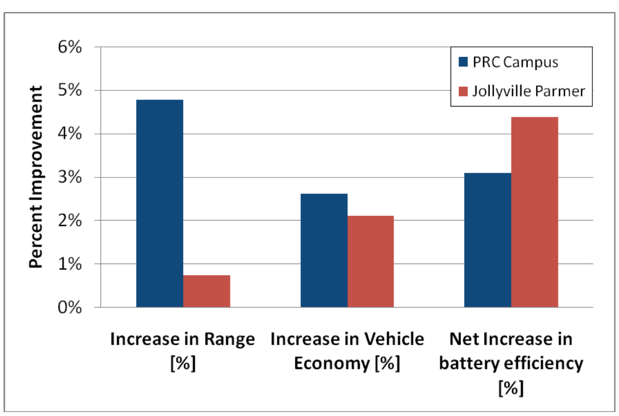

Fig. 14. Predicted performance improvements over the low power PRC Campus route and high power Jollyville Parmer route with additional ultracapacitor energy storage

Acknowledgement

The authors would like to thank the Federal Transit Administration, the Center for Transportation and the Environment, and the Gas Technology Institute for the support of this program.

References

[1] M.M. Flynn, C.S. Hearn, M.C. Lewis, R.C. Thompson, and R.G. Longoria. "Prime Mover and Energy Storage Considerations for a Hydrogen-Powered Series Hybrid Shuttle Bus". Vehicle Power and Propulsion Conference 2007, VPPC 2007, IEEE.

[2] X. He, T. Maxwell, and M. Parten. "Modeling and Validation of a Hydrogen Engine Powered Hybrid Electric Vehicle". Vehicle Power and Propulsion Conference 2007, VPPC 2007, IEEE.

[3] Saft Industrial Battery Group. STM Module, High Energy Nickel-Cadmium Module for Traction Industry. Datasheet, Doc No. 21247-2-0470.

[4] C.S. Hearn. "Modeling of Ultracapacitor and Battery Energy Storage for a Plug-In Hybrid Fuel Cell Shuttle Bus". Master's Thesis submitted to The University of Texas at Austin, December 2008.

[5] A. Burke. "Ultracapacitors: why, how, and where is the technology". Journal of Power Sources, Vol 91, 2000, pp. 37-50..

[6] S.M. Lukic, S.G. Wirasingha, F. Rodrigues, J. Cao, and A. Emadi. "Power Management of an Ultracapacitor/Battery Hybrid Energy Storage System in an HEV". IEEE Vehicle Power and Propulsion Conference, Sept 2006.

[7] J. Park, B. Raju, and A. Emadi. "Effects of an Ultra-Capacitor and Battery Energy Storage System in a Hybrid Electric Vehicle". Future Transportation Technology Conference, Chicago, Il., September 2005. SAE Technical Paper Series 2005-01-3452

[8] A.C. Baisden, and A. Emadi. "ADVISOR-Based Model of a Battery and an Ultracapacitor Energy Source for Hybrid Electric Vehicles". IEEE Transactions on Vehicular Technology, Vol. 53, No. 1, January 2004.

[9] D. Napoli, *et al*. "Design and Testing of a Fuel Cell Powered Propulsion System Supported by a Hybrid UC-Battery Storage". SAE Technical Paper Series 2004-01-1303.

[10] P.C.K Luk and L.C. Rosario, "Power and Energy Management of a Dual Energy Source Electric Vehicle – Policy Implementation Issues". Power Electronics and Motion Control Conference, 2006.